Hydrol. Earth Syst. Sci., 19, 2577–2586, 2015
www.hydrol-earth-syst-sci.net/19/2577/2015/
doi:10.5194/hess-19-2577-2015

Hydrology and Earth System Sciences
Open Access

Seasonal predictions of agro-meteorological drought indicators for the Limpopo basin

F. Wetterhall[1], H. C. Winsemius[2], E. Dutra[1], M. Werner[2,3], and E. Pappenberger[1,4]

[1]European Centre for Medium Range Weather Forecasts, Reading, UK
[2]Deltares, P.O. Box 177, 2600MH, Delft, the Netherlands
[3]UNESCO-IHE, P.O. Box 3015, 2601DA, Delft, the Netherlands
[4]School of Geographical Sciences, University of Bristol, Bristol UK

Correspondence to: F. Wetterhall (fredrik.wetterhall@ecmwf.int)

Received: 22 December 2013 – Published in Hydrol. Earth Syst. Sci. Discuss.: 17 January 2014
Accepted: 21 November 2014 – Published: 2 June 2015

Abstract. The rainfall in southern Africa has a large inter-annual variability, which can cause rain-fed agriculture to fail. The staple crop maize is especially sensitive to dry spells during the early growing season. An early prediction of the probability of dry spells and below normal precipitation can potentially mitigate damages through water management. This paper investigates how well ECMWF's seasonal forecasts predict dry spells over the Limpopo basin during the rainy season December–February (DJF) with lead times from 0 to 4 months. The seasonal forecasts were evaluated against ERA-Interim reanalysis data, which in turn were corrected with GPCP (EGPCP) to match monthly precipitation totals. The seasonal forecasts were also bias-corrected with the EGPCP using quantile mapping as well as post-processed using a precipitation threshold to define a dry day. The results indicate that the forecasts show skill in predicting dry spells in comparison with a climatological ensemble based on previous years. Quantile mapping in combination with a precipitation threshold improved the skill of the forecast. The skill in prediction of dry spells was largest over the most drought-sensitive region. Seasonal forecasts have the potential to be used in a probabilistic forecast system for drought-sensitive crops, though these should be used with caution given the large uncertainties.

1 Introduction

Southern Africa is largely a semi-arid region, which experiences substantial inter- and intra-annual rainfall variability (Barron et al., 2003; Nyakudya and Stroosnijder, 2011). Given the limited extent and scope for development of surface water irrigation, most countries in southern Africa rely strongly on rain-fed agriculture. However, if the rainfall amount or temporal distribution is inadequate, crops may fail, thus compromising food security. While a lower total amount of rainfall over the crop growing season will influence the crop yield, it is often the poor temporal distribution of rainfall resulting in dry spells and wet spells that is the cause of reduced crop yields (Rockstrom, 2000; Ingram et al., 2002; Ochola and Kerkides, 2003; Barron, 2004; Usman and Reason, 2004; Barron and Okwach, 2005).

A staple crop that is grown widely in southeastern Africa is maize, the yields of which are sensitive to the occurrence of dry spells, depending on when these occur. Barron et al. (2003) discuss the sensitivity of maize to the occurrence of dry spells in different stages of the growing season, being particularly high in the first 50 days after sowing, and again during the grain filling stage (70–90 days after sowing). Additionally, the onset of the rains is important, with planting only done after initial rains exceeding 30–40 mm on eight consecutive days in areas studied in Tanzania and Kenya (Barron et al., 2003) and 25 mm on 7 consecutive days or 40 mm on 4 in northern Zimbabwe (Nyakudya and Stroosnijder, 2011). Delays in planting due to late onset of the

Published by Copernicus Publications on behalf of the European Geosciences Union.

rains may result in reduced yield, while planting following a "false" onset of the rain season may lead to failure and the need for expensive replanting. Typical lengths of the growing season for maize are 120–140 days.

Love et al. (2010) summarise a number of typical agro-meteorological indicators that are important for water management and rain-fed agriculture. These hold important information that can aid farmers in improving their agricultural production process, as well as help disaster managers or food security agencies prepare better for food shortage. Examples include the frequency of dry spells of different lengths (Nyakudya and Stroosnijder, 2011), and the probability of the occurrence of dry and wet spells derived from the analysis of historical rainfall through e.g. a Markov chain process (Barron et al., 2003). While these provide valuable information to the understanding of how sensitive (maize) crops in a given area are to reduced yield and even failure, such analysis is useful primarily in the process of the planning of crops and developing of plans for mitigating the impact of dry spells (Kandji et al., 2006).

Reducing the impact of dry and wet spells on the yield may then be found through mitigation measures. Rainfall water harvesting techniques such as improving the soil water retention capacity may reduce vulnerability due to rainfall variability (Brown and Hansen, 2008), and mitigation measures through supplementary irrigation, from for example on-farm ponds (Barron and Okwach, 2005), may reduce the impact of dry spells.

Predictions of dry spells across the growing season and in particular during the periods most sensitive to the impact of dry spells can help plan such mitigation measures, as well as help optimise the use of a scarce commodity such as water stored in on-farm ponds. Additionally, prediction of the onset of the rains can aid a more judicious planning of the sowing period. The importance of the predictability of such indicators, which are tailored to specific end users such as rain-fed agriculture, is acknowledged by Reason et al. (2005). They investigated the inter-annual variability of dry spells within the rainy season, and anomalies in the onset of the rainy season over the Limpopo basin, and found a significant relationship between these indicators and El Nino 3.4 (for a definition, see Trenberth, 1997). The study suggested that there may be predictability of the rainfall characteristics on the seasonal scale within the Limpopo region. Seasonal predictions can be used to inform decisions in planning cropping patterns, planting period, and mitigation measures to reduce the impact of dry spells, or even predict crop yields, such as the sugarcane yield forecasting system proposed by Bezuidenhout and Singels (2007).

Despite the chaotic nature of weather, the potential of seasonal prediction, in particular at the low latitudes, has been long recognised (Charney and Shukla, 1981; Slingo and Palmer, 2011). Useful forecast lead times will also depend very much on the decision that is informed by the prediction. Where decision on cropping patterns would benefit from seasonal forecasts covering the full growing season (120–140 days), or in any case to the end of the grain filling period (90 days), other decisions such as the planning of the sowing period given the onset of the rains, or applying supplemental irrigation may require forecasts with lead times of only up to some 20–30 days.

Such information may be provided by seasonal (0–6 months) forecasting systems. Seasonal forecasts differ from the short-range to medium-range weather forecasts as it does not provide information on the weather on any specific day. Instead, seasonal forecasts provide information on the development of the climate up to 6 months, or in some cases even 12 months ahead. The skill of the seasonal forecasts depends on its ability to model processes at the scale of months, for example the ENSO (El Nino Southern Oscillation). It has to be noted that seasonal forecast systems have significantly more skill than deterministic forecasts (Molteni et al., 2011).

Reason et al. (2005) showed that the December–February (DJF) season is most important because this includes the most crucial periods that influence maize yields, which is particularly sensitive in this season. Moreover, the DJF season is most strongly impacted by ENSO (Lindesay, 1988; Love et al., 2010), which also would result in the best predictability of the rainy season anomalies (Reason et al., 2000; Landman et al., 2001). Winsemius et al. (2014) assessed the ability of ECMWF's seasonal forecasts (SYS4) to predict dry spells and heat stress, indicators relevant to the farmer needs for the Limpopo basin. They found that heat stress was well captured by the seasonal forecasting system, whereas the dry spells were less well captured. A study by Mwangi et al. (2014) further tested the SYS4 for drought forecasting in East Africa and could show skill in the precipitation forecast for the autumn rainy season (September–November).

Forecast models suffer from biases – the climate of the model forecasts differs to a greater or lesser extent from the observed climate. Precipitation is a non-linear and intermittent process, and many atmospheric general circulation models (AGCMs) are not able to correctly resolve these processes, for example, the number of rainy days and heavy precipitation events, due to constraints in resolution and how the processes are implemented in the model. With increasing resolution and better descriptions of model physics the modelling of precipitation will improve in future model versions (Haiden et al., 2014). Since variations in the predicted seasonal distributions are often small, this bias needs to be taken into account, and must be estimated from a previous set of model integrations (Molteni et al., 2011). The 30 year hindcasts of SYS4 provide a large set of forecasts that can be used to correct model biases, and to evaluate the skill of the forecasting system. A common practice is to bias correct the monthly means of the model climate with the verification data set (e.g. Saha et al., 2006).

In this paper we evaluate the skill of the ECMWF seasonal probabilistic forecasting system over the Limpopo basin in southern Africa in predicting indicators relevant to making decisions, within the rainy December–February (DJF) season. Instead of seasonal accumulated anomalies, we tailor this investigation to end user required information on rainfall characteristics, being the length of dry spells and the amount of dry spells within the DJF season. We test how post-processing of the forecast could increase skill depending on the use of quantile mapping against observations and applying a precipitation threshold to define a dry day. The hypothesis is that predictability will increase when a post-processing is applied. The paper is organised as follows: material and methods are described in Sect. 2, the main results in Sect. 3, a discussion in Sect. 4 and main conclusions in Sect. 5.

2 Material and methods

2.1 Study basin

The Limpopo basin (22–25° S, 27–32° E) land use is governed by croplands, in particular in the downstream (i.e. eastern) part of the basin (Fig. 1). Most of these croplands are rain-fed or rely on the scarce and over-committed surface water resources (Love et al., 2010). The climate is characterised by extremely variable rainfall, resulting in a mixture of very dry years and years with floods. Rainfall concentrates in one rainy season, largely controlled by the Inter-Tropical Convergence Zone, which means that most of the rainfall is received in the months December, January and February (DJF). The precipitation in Limpopo is very dependent on ENSO giving warm and dry years during strong ENSO events (Ogallo, 1988). Its water resources are shared by South Africa, Botswana, Zimbabwe and Mozambique. There are a number of important water users in the basin, amongst which are ecology and nature preservation (a large part of the Kruger National Park is located inside the basin), municipalities, agriculture and livestock. The agricultural users (except some large corporate sugarcane fields in the South African part of the basin) are primarily smallholder farmers, without access to significant supplementary irrigation.

The Limpopo basin suffers from drought every 7 to 11 years, but there are large differences in vulnerability to droughts, as shown in the Drought Hazard Index (DHI) maps (Fig. 2; Muñoz Leira et al., 2003). The DHI maps show the probability of crop failure combined with the degree of rainfall variability from year to year, and a low (high) DHI means a stable (sensitive) environment. Four regions were identified according to their geographical location and drought hazard: regions 1 and 3 with moderate to high; region 2 with high/very high; and region 4 with low/moderate DHI respectively. The analysis in this study was made for the catchment as a whole and for each region separately.

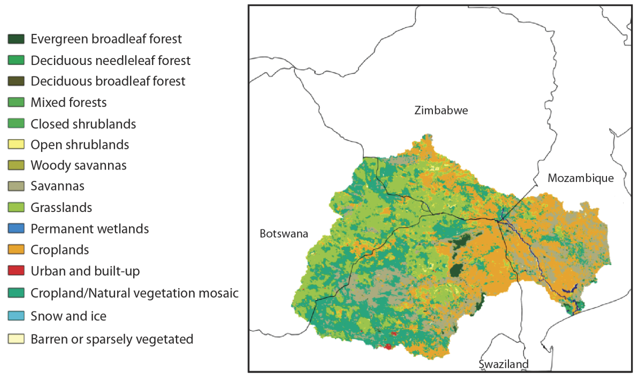

Figure 1. Land use in the Limpopo River basin (source: IGBP; Loveland et al., 2000). The orange coloured regions are classified as croplands, most of which are rain-fed.

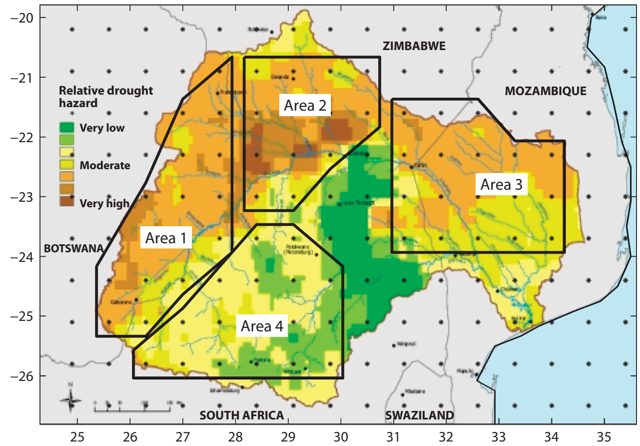

Figure 2. Areas of drought hazard for the Limpopo basin. The four areas are characterised by their sensitivity to droughts, ranging from low/moderate to very high/high. The underlying maps are from Muñoz Leira et al. (2003). The grid points denote the grid points of the ECMWF seasonal forecasting system (SYS4) on a T319 reduced Gaussian grid.

2.2 Data description

2.2.1 Merged ERA-Interim and GPCP rainfall estimates

ERA-Interim (hereafter ERAI) is the latest global atmospheric reanalysis produced by ECMWF. ERAI covers the period from 1 January 1979 onwards, and continues to be extended forward in near-real time (www.ecmwf.int; Dee et al., 2011). The ERAI configuration has a spectral T255 horizontal resolution, which corresponds to approximately 79 km. ERAI suffers from model biases, and to correct precipitation, Balsamo et al. (2010) performed a scale-selective rescaling, hereafter named EGPCP. The procedure corrected ERAI 3-hourly precipitation on a grid-point scale with multiplicative factors to match the total monthly accumulation of the GPCP v2.1 product (Huffman et al., 2009). The advantage of this procedure is that small-scale features of ERAI can be preserved (e.g. orographic precipitation enhancement) while the monthly totals are rescaled to match GPCP. Moreover, the rescaling improves the root mean square error and spatial/temporal correlations by combining the advantages of the observation-based GPCP product with those of the original high-resolution ERAI data. Szczypta et al. (2011) evaluated ERAI over France, based on the high-resolution (8 km) SAFRAN atmospheric reanalysis (Vidal et al., 2010), and found that the EGPCP precipitation performs better than the original ERAI product. Belo-Pereira et al. (2011) compared the skill of ERAI and GPCC (similar to GPCP over land), among others, against a high-resolution observational-based data set of precipitation. They found that both ERAI and GPCP provided a good estimate of drought conditions, the latter closer to the observations. The merged EGPCP rainfall estimate is assumed to be the best estimation of ground truth in this study. All skill evaluations are therefore based on comparisons between seasonal forecast and the EGPCP estimates.

2.2.2 ECMWF seasonal forecast system

The ECMWF seasonal forecasts system 4 (SYS4) consists of a global coupled ocean–atmosphere general circulation model to calculate the evolution of the ocean and atmosphere and an ocean analysis to estimate the initial state of the ocean (Molteni et al., 2011). The ocean model used is NEMO (Nucleus for European Modelling of the Ocean; Madec, 2012) adopting the ORCA1 grid, which has a horizontal resolution of approximately 1°, and 42 levels in the vertical (http://www.noc.soton.ac.uk/nemo/?page=configurations, last access 3 December 2014). The atmospheric component of SYS4 is the ECMWF integrated forecasts system (IFS) with the same horizontal resolution is the same as ERAI but using 91 vertical levels instead of the 60 used in ERAI. The forecasts consist of a 51 member ensemble, with initial date of the 1st of each month, and then run daily for 7 months. The 51 ensemble members are made up with one control member initialised by ERA-Interim and 50 ensembles in which the initial conditions (ocean and atmosphere) combined with stochastic schemes in the model physics of the atmospheric model. The re-forecasts (also referred to as hindcasts) for SYS4 consist of forecasts starting on the 1st of every month for the years 1981–2010 with an ensemble size of 15 members. The hindcasts can be used to calibrate the real-time forecasts in combination with the observed weather and climate.

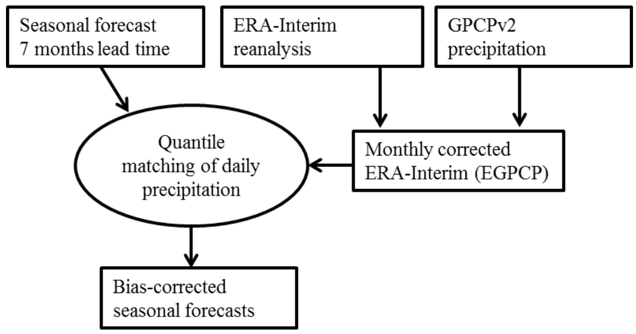

Figure 3. Flowchart of the bias correction of the seasonal forecasts.

2.3 Experimental setup

2.3.1 Quantile-based mapping

In this study we evaluate dry spells based on daily precipitation, and a simple mean monthly bias correction would not correct biases in the distribution of dry events. Therefore a quantile-based mapping (QM; Panofsky and Brier, 1968) was applied on the forecast. QM adjusts the forecasted precipitation to the observed precipitation (in our case EGCP) by matching the cumulative density function (CDF) of daily precipitation for each grid cell individually. This relatively simple approach has been successfully used in hydrological and climate impact studies (e.g. Maurer and Hidalgo, 2008; Li et al., 2010; Jakob Themeßl et al., 2011; Wetterhall et al., 2012) as well as medium-range (Voisin et al., 2010) and seasonal forecasts (Wood et al., 2002). The precipitation of the seasonal forecast was rescaled using a multiplicative factor (or transfer function) for each initial forecast date (calendar month), lead time and grid point. The multiplicative factor is a discrete array which corrects the precipitation values for quantiles ranging from 0 to 1 with a step of 0.02. QM was only done for rainy days since the number of rainy days are very similar for the SYS4 and EGPCP, and therefore an adjustment of the number of rainy days was not necessary. A schematic view of the corrections used in this paper is shown in Fig. 3.

To account for the uncertainty due to the small sample size, the CDFs of the hindcasts of SYS4 and EGPCP were evaluated empirically by sorting the daily precipitation and then bootstrapping 50 distributions from a sample of 50 % of the data, thereby creating 50 SYS4 CDFs and their respective multiplicative factors. The final correction used the average of the 50 bootstrapped multiplicative factors to adjust the distribution. To allow a smooth transition in time of the multiplicative factor, and to increase the sample size, the training data set was expanded using the two adjacent months for each lead time. For example, for the forecasts starting in November with lead time 1 (valid in December), we selected all the November, December and January months from EGPCP, and the SYS4 forecasts starting in November for lead

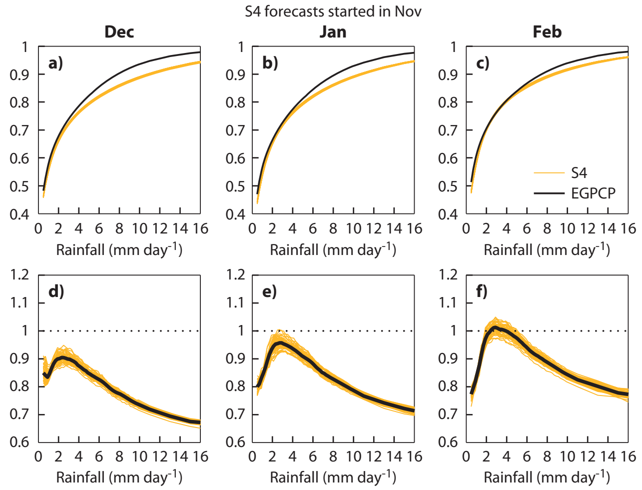

Figure 4. Cumulative density function (CDF) **(a–c)** of daily precipitation from EGPCP (black) and SYS4 forecasts started in November (grey lines from the bootstrapping sampling) and valid for December **(a)**, January **(b)** and February **(c)**. Quantile match coefficients applied to correct SYS4 forecasts (black mean, grey bootstrapping range) started in November and valid in December **(d)**, January **(e)** and February **(f)**. The represented CDFs and quantile match coefficients were averaged over the region (27 to 32° E; −22 to −25° N).

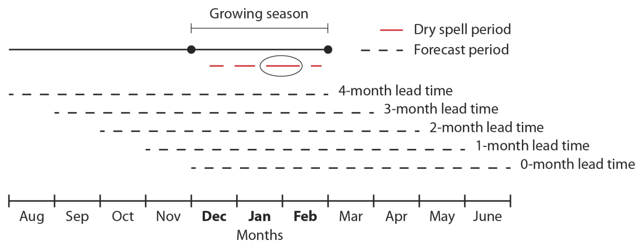

Figure 5. The timing of the growing season and lead times of seasonal forecasts. Evaluation of dry spells is performed in the growing season (see red lines).

times 0, 1 and 2 to evaluate the empirical CDFs (Fig. 4). To make the comparison easier, both the EGCP and SYS4 data were interpolated to a regular grid with spatial resolution 0.7° in latitude and longitude, which is very close to the original resolution of the seasonal forecasts.

2.3.2 Skill as function of dry/wet day threshold, bias correction, spatial scale and lead time

The predictability of the occurrence of dry spells and dry spell length can be assumed to be dependent on the following factors: (1) the lead time of the seasonal forecast, (2) the definition of a dry day within the perspective of our meteorological forecast model, (3) the presence of model bias (which in itself is also assumed to be a function of lead time) and (4) the spatial averaging scale of prediction. ECMWF's seasonal forecasting system archives daily forecasts with a lead time of 7 months, starting at the first day of each month. Subsequently, five forecasts overlap the rainy season (DJF) any given year, with lead times with respect to the onset of DJF season ranging from 0 to 4 months. There is large evidence that seasonal forecast skill deteriorates strongly with lead time (Molteni et al., 2011). Therefore, the forecast was evaluated for each lead time.

In this study a "dry spell" was defined as a sequence of days (minimum 3 days) where rainfall is below a certain threshold (see the red bars in Fig. 5). The threshold accounts for a number of factors, for example that part of a day's rainfall is intercepted by canopy, understory, litter and by the very top few centimetres of soil; and therefore evaporates before infiltrating down to the root zone (Savenije, 2004; de Groen and Savenije, 2006; Gerrits et al., 2007). This amount can be significant, and De Groen and Savenije (2006) suggest a value between 2 and 5 mm day^{-1} for the southern African region, depending on season and land cover characteristics. These water balance components therefore do not take part in the biomass assimilation process and from the point of view of a crop, a day is therefore wet as soon as rainfall exceeds a certain threshold. To test the sensitivity of the choice of this threshold, a large range of thresholds were considered, ranging from 1 to 15 mm day^{-1}. Note that from the point of view of crop growth, 15 mm day^{-1} rainfall should not be considered to be a dry day anymore (de Groen and Savenije, 2006). The wide range is only used to demonstrate the predictability of the ECMWF probabilistic seasonal forecasting system over a range of thresholds. For each forecast, the frequency of dry spells, defined as the number of dry spells longer than 3 days, was computed for each model grid cell. The same was done for the observational data EGPCP. This results in pairs of "observed" and forecast values for the frequency of dry spells and the length of the longest dry spell for each lead time and for each year of available data.

2.3.3 Computation of skill measures

Relative operating characteristic (ROC) and continuous ranked probability scores (CRPS; Matheson and Winkler, 1976) were used to estimate the performance of SYS4. The correlation coefficient was calculated on the annual averages of the all ensemble members and all the land grid points in the Limpopo basin compared with EGCP. The hits, misses and false alarms for the contingency table were estimated by considering values above the 70th percentile of the EGCP data as an event. The contingency table was calculated over all grid points and ensemble members and then averaged into hit rates (HR) and false alarm rates (FAR).

$$\mathrm{HR} = \frac{\mathrm{Hits}}{\mathrm{Hits} + \mathrm{Misses}} \tag{1}$$

$$\mathrm{FAR} = \frac{\mathrm{False\ alarms}}{\mathrm{False\ alarms} + \mathrm{Correct\ negatives}} \tag{2}$$

Plotting the FAR against HR for various thresholds of detection, i.e. the probability of an event generates the receiver operating characteristic (ROC) curve, from which the area under the ROC curve (AUC) can be estimated. The AUC is a summary statistics of the performance of the system and tests the system's ability to discriminate between positive and negative outcomes. A value of AUC close to 1 denotes a perfect forecast, whereas values below 0.5 denote that the forecast performs worse than a random forecast.

CRPS is a common tool to evaluate ensemble data and is defined as

$$\mathrm{CRPS} = \frac{1}{N}\sum_{n=1}^{N}\int_{-\infty}^{\infty}\left[F(x) - H(x - x_0)^2\right]\mathrm{d}x, \tag{3}$$

where N is the number of forecasts, $F(x)$ is the cumulative distribution function $F(x) = p(X \leq x)$ of the forecasted precipitation x, x_o the observed precipitation, and $H(x–x_0)$ is the Heaviside function, which has the value 0 when $x–x_0 < 0$ and 1 otherwise. In order to quantify the skill of the probability score, the skill score is calculated as

$$\mathrm{SS_{CRPS}} = 1 - \frac{\mathrm{CRPS_{FP}}}{\mathrm{CRPS_{RP}}}, \tag{4}$$

where $\mathrm{CRPS_{FP}}$ denotes the forecast score and $\mathrm{CRPS_{RP}}$ is the score of a reference forecast of the same predictand. CRPS and $\mathrm{SS_{CRPS}}$ were calculated for each grid point and lead time respectively. The benchmark forecast in this study was a climatological ensemble, which was created by randomly selecting 15 time series (to match the seasonal forecast hindcast ensemble size) from each starting month from the EGPCP historical database of the same length as the seasonal forecast (7 months), excluding the actual year.

3 Results

The results from the hindcast period were evaluated in terms of the effect of the precipitation threshold and bias correction. Furthermore, the predictability for the four identified regions was evaluated individually.

3.1 Effect of quantile mapping

The forecast of frequencies and length of the longest dry spell were both improved in absolute terms, which is to be expected since the correction is towards observed values (Table 1). The bias correction affected both hit rates and false alarms but in opposite directions, depending on the target variable; hits and false alarms increased (decreased) for the length of the longest dry spell (frequency of dry spells). The overall effect on AUC was however an improvement (or no effect) after QM. The positive effect of the QM becomes more apparent with the increasing precipitation threshold (Fig. 6). The boxplots indicate the inter-annual spread in the EGPCP data, and this is substantially larger than for the forecast, which is also seen in Table 1. There is a breakpoint around 5 mm, where the forecast and the EGCP data show the best agreement, and the effect of the QM persists with increasing thresholds. Figure 6 shows the result for lead time 0, but the results are similar for longer lead times (not shown).

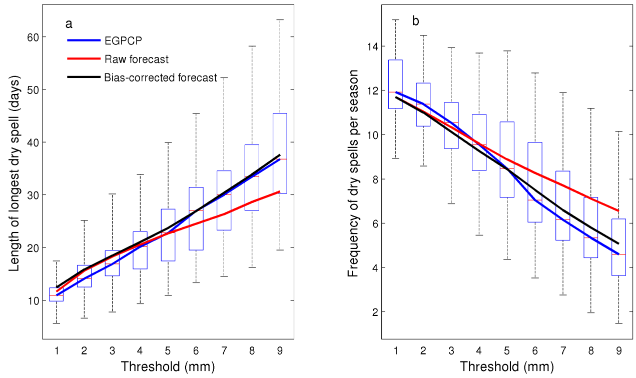

Figure 6. Effect of the threshold on **(a)** the length of dry spells and **(b)** frequency of dry spells for EGPCP, raw forecast and bias-corrected forecast for each season over the entire forecast period for lead time 0. The edges of the boxplot show the 25 and 75 quantiles; the whiskers indicate the maximum and minimum values.

3.2 Skill as function of precipitation thresholds

Using a non-zero threshold to define rainy and non-rainy days has a clear impact on the skill (Fig. 7). The effect of the thresholds is different for the raw and corrected forecast. Using a threshold of precipitation of between 5 and 10 mm depending on lead time and target variable was the optimum for the bias-corrected forecasts, whereas the optimum threshold for the raw forecast was lower. However, a threshold of 10 mm is higher than the precipitation amounts expected to be lost to transpiration from interception. To accommodate for the most optimum threshold as well as to use a physically sensible threshold, 5 mm was selected, which is in agreement with previous studies (de Groen and Savenije, 2006).

3.3 Spatial variations in skill

The spatial pattern of skill for the raw forecast shows a pattern where the forecast performance of the south-western part of the Limpopo catchment is comparatively worse than for the north-east (Fig. 8). The patterns are similar for both the longest dry spell and the frequency of dry spells. QM im-

Table 1. Length of dry spells and frequency of dry spells from the EGCP data (observed) and forecasted with raw forecast and bias corrected. The results are with a 5 mm threshold applied and averaged over all points and years, and all ensemble members for the forecast. The standard deviation is shown in brackets.

	Lead 1	Lead 2	Lead 3	Lead 4	Lead 5
Frequencies of dry spells					
Observed	8.7 (2.2)				
Raw forecast	9.0 (1.1)	9.2 (1.1)	9.4 (0.8)	9.5 (0.9)	9.6 (0.7)
Corrected forecast	8.5 (1.1)	8.7 (1.1)	8.8 (0.9)	8.8 0.9)	8.7 (0.7)
AUC raw	0.67	0.63	0.56	0.58	0.58
AUC corrected	0.69	0.65	0.59	0.61	0.59
Length of longest dry spells					
Observed	23 (7.4)				
Raw forecast	23 (3.0)	22 (3.2)	21 (2.3)	21 (2.2)	20 (1.9)
Corrected forecast	24 (3.3)	23 (3.5)	23 (2.5)	23 (2.4)	23 (2.1)
AUC raw	0.54	0.55	0.51	0.52	0.55
AUC corrected	0.58	0.55	0.51	0.53	0.55

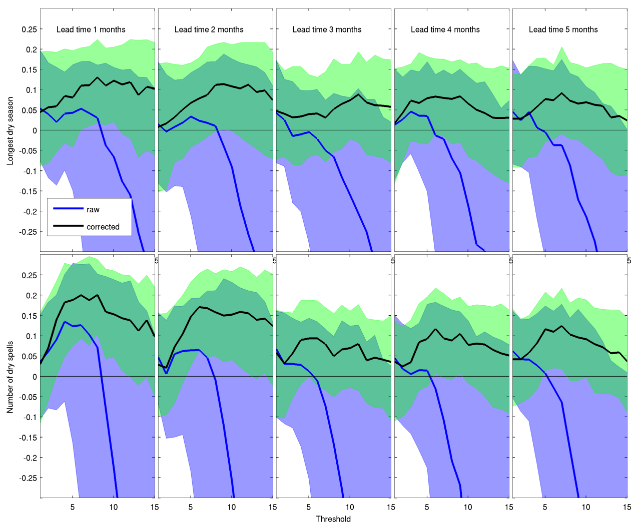

Figure 7. CRPSS as a function of precipitation thresholds for different lead times over the Limpopo catchment. Top panel shows the results for the longest dry spell over the rainy season, and the bottom panel the frequency of dry spells over the rainy season. The blue line denotes the raw forecast, and the black line the bias-corrected. The blue (green) areas denote the 5 to 95 spread of the raw (corrected) forecasts respectively.

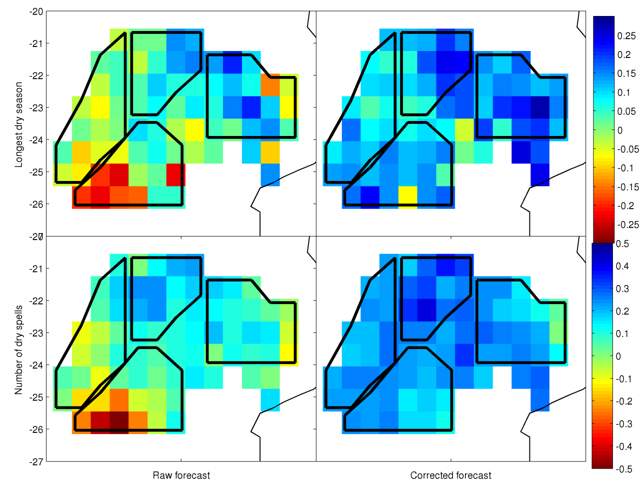

Figure 8. CRPSS for the different areas over the Limpopo basin with a precipitation threshold of 5 mm and lead time of 1 month.

proved the forecast over all grid boxes and the increase is largest for the shorter lead times (Fig. 9). The highest skill both before and after the QM was seen for area 2, which is also the most vulnerable to droughts. The forecasts for area 4, which also is the area least sensitive to droughts, had the lowest skill. The correction improved the skill scores to levels comparable to the other areas. The effect of QM is most evident for the shorter lead times; for the longer lead times, the signal is noisier.

4 Discussion

4.1 Choices in the methodology

It was found very useful to perform a proper bias correction of the forecasts before any attempt was made to predict the occurrence and length of dry spells. This is demonstrated by comparing bias-corrected skill with non-bias-corrected skill (Figs. 5–8). The CRPSS was in many cases negative prior to QM. The computation of dry spells and dry periods is strongly dependent on the ability of the prediction system to distinguish a wet day from a dry day, and the seasonal forecasts are typically impacted by significant bias during low-intensity rainfall ("drizzle effect"), which strongly impacts

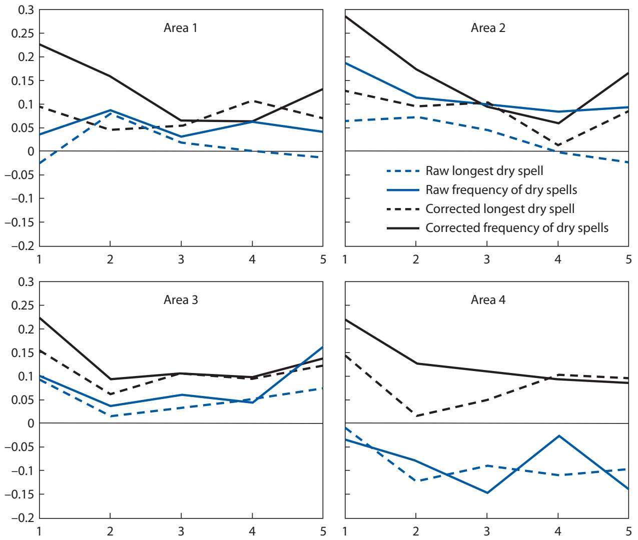

Figure 9. CRPSS as a function of lead time for the four areas in the Limpopo basin.

on the lower tail of the distribution of the forecasted daily rainfall amount.

The effect of the variable threshold on the definition of dry spells creates fewer but longer dry spells with increasing threshold. It targets the effective precipitation, which is the precipitation that is available for plants. The application of a threshold precipitation at which a dry spell was defined improved the results, especially after QM, which would suggest that using both methods in combination was necessary to optimise the performance of the forecast. Since the simple bias correction only affected the amount of precipitation, the effect of the threshold is more visible on the higher end of the distribution. The selection of the optimal threshold is in the end dependent on the application, i.e. what is most important for the crop in terms of water need. The results in this study shows that the bias correction has a positive effect on all thresholds in the range from 1 to 15 mm. The threshold can also be applied prior to applying bias correction (e.g. Wetterhall et al., 2012), but in cases where the energy balance is important, for example in cases where agriculture production is to be modelled, a correction of the temperature distribution would also be needed, since the occurrence or non-occurrence of precipitation will affect the modelled temperature. The advantage of the methodology used in this study is that the spatial correlation between temperature and precipitation is better preserved.

The skill of the forecast varies generally significantly with location, and this is clear also from our study. The highest skill for the raw forecast was found in the northern part of the catchment. However, the potential predictive skill of SYS4 is more or less equal across the catchment, as is demonstrated by the effect on the post-processing of the forecasts (Figs. 8–9). The potential skill is in this paper evaluated using GPCP v2.2 as the "ground truth"; however, this has its limitations, as the quality of this global data set is very varying. If the true skill of the system is to be assessed, local station precipitation data would be necessary. However, as a proof-of-concept, the proposed methodology is promising.

4.2 Potential value of the forecasting of rainfall characteristics

Although seasonal forecasts deliver to some degree skilful information on dry spell occurrence and dry spell lengths, it is not guaranteed that this information will improve the decision making process for the end user. Translation from a forecast has value if the decisions that are taken based on the forecast information indeed lead to an effective gain (whether this is monetary or in some other way) with respect to the status quo (i.e. without a forecast being used for decision making). This is only the case if the integral of costs (monetary or in any other meaningful form) of additional actions being taken on the basis of the forecast information over time is lower than the integral of loss, prevented by the alternate decision. This has been demonstrated by Verkade and Werner (2011) for the case of flood forecasting and warning systems (Verkade and Werner, 2011; Pappenberger et al., 2015). In most forecasting evaluations, the costs associated with the decision and actions following this decision are neglected, meaning that if the forecast has any skill compared to the climatology, the system always has value. However, if such costs cannot be neglected, then the value of the forecast will decrease depending on the rate of false alarms and misses. A false alarm will result in unnecessary costs, being made to decide and act, while a hit will result in prevented losses, which obviously are higher than the costs to act. In order to evaluate the value of this forecast, we would therefore require local knowledge about how much the action, followed by a forecast warning (in the case of the Limpopo, importing of food and fodder) would cost, and how much would be lost due to the occurrence of (long) dry spells, if action would have been required, but is not taken. In the Limpopo case, this could involve loss of harvest, loss of livestock, or even loss of lives if food security is at stake.

5 Conclusions

This paper assesses the quality of using seasonal forecasts from ECMWF to predict the duration of the longest dry spell as well as the frequency of dry spells during the growing season in the Limpopo basin in southeastern Africa. The paper further investigates post-processing techniques of the forecasts by applying a QM of the forecasts and a precipitation threshold to define wet and dry events. The threshold was applied to both the observed data and forecast to test the sensitivity to user-defined needs. The results show that the forecasts are improved by using a threshold to define events in combination with QM of the forecast. Post-processing increases the potential predictability of the forecasts, but in order to assess the full added value of a forecasting system, it would need to be tested as a decision support tool by local stakeholders.

Acknowledgements. This work was funded by the FP7 EU projects DEWFORA EU FP-7, grant agreement number 265454 (http://www.dewfora.net), and GLOWASIS (http://www.glowasis.eu). We thank the two anonymous reviewers for their valuable comments and suggestions.

Edited by: L. Samaniego

References

Balsamo, G., Boussetta, S., Lopez, P., and Ferranti, L.: Evaluation of ERA-Interim and ERA-Interim-GPCP-rescaled precipitation over the U.S.A, European Centre for Medium Range Weather Forecasts, Reading, UK, 10, 2010.

Barron, J.: Dry spell mitigation to upgrade semi-arid rainfed agriculture: Water harvesting and soil nutrient management for smallholder maize cultivation in Machakos, Kenya, Doctoral thesis, comprehensive summary, PhD, Stockholm University, Stockholm, 2004.

Barron, J. and Okwach, G.: Run-off water harvesting for dry spell mitigation in maize (Zea mays L.): results from on-farm research in semi-arid Kenya, Agr. Water Manage., 74, 1–21, doi:10.1016/j.agwat.2004.11.002, 2005.

Barron, J., Rockström, J., Gichuki, F., and Hatibu, N.: Dry spell analysis and maize yields for two semi-arid locations in east Africa, Agr. Forest Meteorol., 117, 23–37, doi:10.1016/S0168-1923(03)00037-6, 2003.

Belo-Pereira, M., Dutra, E., and Viterbo, P.: Evaluation of global precipitation data sets over the Iberian Peninsula, J. Geophys. Res.-Atmos., 116, 2156–2202, doi:10.1029/2010JD015481, 2011.

Bezuidenhout, C. N. and Singels, A.: Operational forecasting of South African sugarcane production: Part 1 – System description, Agr. Syst., 92, 23–38, doi:10.1016/j.agsy.2006.02.001, 2007.

Brown, C. and Hansen, J. W.: Agricultural Water Management and Climate Risk, International Research Institute for Climate and Society, Palisades, New York, USA, 19, 2008.

Charney, J. G. and Shukla, J.: Predictability of monsoons, in: Monsoon dynamics, edited by: Lighthill, S. J. and Pearce, R. P., Cambridge University Press., Cambridge, UK, 99–110, 1981.

Dee, D. P., Uppala, S. M., Simmons, A. J., Berrisford, P., Poli, P., Kobayashi, S., Andrae, U., Balmaseda, M. A., Balsamo, G., Bauer, P., Bechtold, P., Beljaars, A. C. M., van de Berg, L., Bidlot, J., Bormann, N., Delsol, C., Dragani, R., Fuentes, M., Geer, A. J., Haimberger, L., Healy, S. B., Hersbach, H., Hólm, E. V., Isaksen, L., Kållberg, P., Köhler, M., Matricardi, M., McNally, A. P., Monge-Sanz, B. M., Morcrette, J. J., Park, B. K., Peubey, C., de Rosnay, P., Tavolato, C., Thépaut, J. N., and Vitart, F.: The ERA-Interim reanalysis: configuration and performance of the data assimilation system, Q. J. Roy. Meteorol. Soc., 137, 553–597, doi:10.1002/qj.828, 2011.

de Groen, M. M. and Savenije, H. H. G.: A monthly interception equation based on the statistical characteristics of daily rainfall, Water Resour. Res., 42, W12417, doi:10.1029/2006WR005013, 2006.

Gerrits, A. M. J., Savenije, H. H. G., Hoffmann, L., and Pfister, L.: New technique to measure forest floor interception – an application in a beech forest in Luxembourg, Hydrol. Earth Syst. Sci., 11, 695–701, doi:10.5194/hess-11-695-2007, 2007.

Haiden, T., Magnusson, L., Tsonevsky, I., Wetterhall, F., Alfieri, L., Pappenberger, F., de Rosnay, P., Muñoz-Sabater, J., Balsamo, G., Albergel, C., Forbes, R., Hewson, T., Malardel, S., and Richardson, D.: ECMWF forecast performance during the June 2013 flood in Central Europe, Euopean Centre for Medium-Range Weather Forecasts, Reading, United Kingdom, 34, 2014.

Huffman, G. J., Adler, R. F., Bolvin, D. T., and Gu, G.: Improving the global precipitation record: GPCP Version 2.1, Geophys. Res. Lett., 36, L17808, doi:10.1029/2009GL040000, 2009.

Ingram, K. T., Roncoli, M. C., and Kirshen, P. H.: Opportunities and constraints for farmers of west Africa to use seasonal precipitation forecasts with Burkina Faso as a case study, Agri. Syst., 74, 331–349, 2002.

Jakob Themeßl, M., Gobiet, A., and Leuprecht, A.: Empirical-statistical downscaling and error correction of daily precipitation from regional climate models, Int. J. Climatol., 31, 1530–1544, doi:10.1002/joc.2168, 2011.

Kandji, S. T., Verchot, L., and Mackensen, J.: Climate Change and Variability in the Sahel Region: Impacts and Adaptation Strategies in the Agricultural Sector, World Agroforestry Centre (ICRAF) United Nations Environment Programme (UNEP), Nairobi, Kenya, 48, 2006.

Landman, W. A., Mason, S. J., Tyson, P. D., and Tennant, W. J.: Retro-active skill of multi-tiered forecasts of summer rainfall over southern Africa, Int. J. Climatol., 21, 1–19, doi:10.1002/joc.592, 2001.

Li, H., Sheffield, J., and Wood, E. F.: Bias correction of monthly precipitation and temperature fields from Intergovernmental Panel on Climate Change AR4 models using equidistant quantile matching, J. Geophys. Res.-Atmos. (1984–2012), 115, 1984–2012, doi:10.1029/2009JD012882, 2010.

Lindesay, J. A.: South African rainfall, the Southern Oscillation and a Southern Hemisphere semi-annual cycle, J. Climatol., 8, 17–30, doi:10.1002/joc.3370080103, 1988.

Love, D., Uhlenbrook, S., Twomlow, S., and Zaag, P. v. d.: Changing hydroclimatic and discharge patterns in the northern Limpopo Basin, Zimbabwe, Water SA, 36, 335–350, 2010.

Loveland, T. R., Reed, B. C., Brown, J. F., Ohlen, D. O., Zhu, Z., Yang, L., and Merchant, J. W.: Development of a global land cover characteristics database and IGBP DISCover from 1 km AVHRR data, Int. J. Remote Sens., 21, 1303–1330, doi:10.1080/014311600210191, 2000.

Madec, G.: NEMO ocean engine, Note du P^ole de mod’elisation de l’Institut Pierre-Simon Laplace No 27, Paris, FranceISSN No 1288-1619, 2012.

Matheson, J. E. and Winkler, R. L.: Scoring Rules for Continuous Probability Distributions, Manage. Sci., 22, 1087–1096, doi:10.1287/mnsc.22.10.1087, 1976.

Maurer, E. P. and Hidalgo, H. G.: Utility of daily vs. monthly large-scale climate data: an intercomparison of two statistical downscaling methods, Hydrol. Earth Syst. Sci., 12, 551–563, doi:10.5194/hess-12-551-2008, 2008.

Molteni, F., Stockdale, T., Balmaseda, M., Balsamo, G., Buizza, R., Ferranti, L., Magnusson, L., Mogensen, K., Palmer, T., and Vitart, F.: The new ECMWF seasonal forecast system (System 4), ECMWF, Reading, United Kingdom, 49, 2011.

Muñoz Leira, E., Landis, R., Alberto, J., Machava, E., Enoque, E. E., and Chauque, L.: Atlas for disaster preparedness and response in the Limpopo Basin, in, WorldCat, available at: http://edmc1.dwaf.gov.za/library/limpopo/ (last access: 1 December 2014), 2003.

Mwangi, E., Wetterhall, F., Dutra, E., Di Giuseppe, F., and Pappenberger, F.: Forecasting droughts in East Africa, Hydrol. Earth Syst. Sci., 18, 611–620, doi:10.5194/hess-18-611-2014, 2014.

Nyakudya, I. W. and Stroosnijder, L.: Water management options based on rainfall analysis for rainfed maize (Zea mays L.) production in Rushinga district, Zimbabwe, Agr. Water Manage., 98, 1649–1659, doi:10.1016/j.agwat.2011.06.002, 2011.

Ochola, W. O. and Kerkides, P.: A Markov chain simulation model for predicting critical wet and dry spells in Kenya: analysing rainfall events in the Kano Plains, Irrig. Drainage, 52, 327–342, doi:10.1002/ird.94, 2003.

Ogallo, L. J.: Relationships between seasonal rainfall in East Africa and the Southern Oscillation, J. Climatol., 8, 31–43, doi:10.1002/joc.3370080104, 1988.

Panofsky, H. A. and Brier, G. W.: Some Applications of Statistics to Meteorology, Earth and Mineral Sciences Continuing Education, College of Earth and Mineral Sciences, Pennsylvania, USA, 224 pp., 1968.

Pappenberger, F., Cloke, H. L., Parker, D. J., Wetterhall, F., Richardson, D. S., and Thielen, J.: The monetary benefit of early flood warnings in Europe, Environ. Sci. Pol., 51, 278–291, doi:10.1016/j.envsci.2015.04.016, 2015.

Reason, C. J. C., Allan, R. J., Lindesay, J. A., and Ansell, T. J.: ENSO and climatic signals across the Indian Ocean Basin in the global context: part I, interannual composite patterns, Int. J. Climatol., 20, 1285-1327, doi:10.1002/1097-0088(200009)20:11<1285::AID-JOC536>3.0.CO;2-R, 2000.

Reason, C. J. C., Hachigonta, S., and Phaladi, R. F.: Interannual variability in rainy season characteristics over the Limpopo region of southern Africa, Int. J. Climatol., 25, 1835–1853, doi:10.1002/joc.1228, 2005.

Rockstrom, J.: Water resources management in smallholder farms in Eastern and Southern Africa: An overview, Phys. Chem. Earth, Part B: Hydrology, Oceans and Atmosphere, 25, 275–283, doi:10.1016/S1464-1909(00)00015-0, 2000.

Saha, S., Nadiga, S., Thiaw, C., Wang, J., Wang, W., Zhang, Q., Van den Dool, H. M., Pan, H. L., Moorthi, S., Behringer, D., Stokes, D., Peña, M., Lord, S., White, G., Ebisuzaki, W., Peng, P., and Xie, P.: The NCEP Climate Forecast System, J. Climate, 19, 3483–3517, doi:10.1175/JCLI3812.1, 2006.

Savenije, H. H. G.: The importance of interception and why we should delete the term evapotranspiration from our vocabulary, Hydrol. Process., 18, 1507–1511, doi:10.1002/hyp.5563, 2004.

Slingo, J. and Palmer, T.: Uncertainty in weather and climate prediction, Philos. Trans. Roy. Soc. A: Mathematical, Physical and Engineering Sciences, 369, 4751–4767, doi:10.1098/rsta.2011.0161, 2011.

Szczypta, C., Calvet, J.-C., Albergel, C., Balsamo, G., Boussetta, S., Carrer, D., Lafont, S., and Meurey, C.: Verification of the new ECMWF ERA-Interim reanalysis over France, Hydrol. Earth Syst. Sci., 15, 647–666, doi:10.5194/hess-15-647-2011, 2011.

The NOCS ORCA1 home page, available at: http://www.noc.soton.ac.uk/nemo/?page=configurations, last access: 3 December 2014.

Trenberth, K. E.: The Definition of El Niño, B. Am. Meteorol. Soc., 78, 2771–2777, doi:10.1175/1520-0477(1997)078<2771:TDOENO>2.0.CO;2, 1997.

Usman, M. T. and Reason, C. J. C.: Dry spell frequencies and their variability over southern Africa, Clim. Res., 26, 199–211, doi:10.3354/cr026199, 2004.

Verkade, J. S. and Werner, M. G. F.: Estimating the benefits of single value and probability forecasting for flood warning, Hydrol. Earth Syst. Sci., 15, 3751–3765, doi:10.5194/hess-15-3751-2011, 2011.

Vidal, J. P., Martin, E., Franchistéguy, L., Baillon, M., and Soubeyroux, J.-M.: A 50-year high-resolution atmospheric reanalysis over France with the Safran system, Int. J. Climatol., 30, 1627–1644, doi:10.1002/joc.2003, 2010.

Voisin, N., Schaake, J., and Lettenmaier, D. P.: Calibration and Downscaling Methods for Quantitative Ensemble Precipitation Forecasts, Weather Forecast., 25, 1603–1627, 2010.

Wetterhall, F., Pappenberger, F., He, Y., Freer, J., and Cloke, H. L.: Conditioning model output statistics of regional climate model precipitation on circulation patterns, Nonlin. Processes Geophys., 19, 623–633, doi:10.5194/npg-19-623-2012, 2012.

Winsemius, H. C., Dutra, E., Engelbrecht, F. A., Archer Van Garderen, E., Wetterhall, F., Pappenberger, F., and Werner, M. G. F.: The potential value of seasonal forecasts in a changing climate in southern Africa, Hydrol. Earth Syst. Sci., 18, 1525–1538, doi:10.5194/hess-18-1525-2014, 2014.

Wood, A. W., Maurer, E. P., Kumar, A., and Lettenmaier, D. P.: Long-range experimental hydrologic forecasting for the eastern United States, J. Geophys. Res.-Atmos., 107, 4429, doi:10.1029/2001JD000659, 2002.